



*Research article*

## **Bioinformatics modeling for KLF2-Binding downstream promoter motifs of cytotoxic T-cell regulation**

**Jason Chengwu Duan<sup>1</sup>, Wenqin Li<sup>2</sup> and Biaoru Li<sup>3,\*</sup>**

<sup>1</sup> Department of Biostatistics, University of California, Los Angeles, CA, USA

<sup>2</sup> Department of Chemistry, University of California, Irvine, CA 92697, USA

<sup>3</sup> Senior Faculty of Principal Research Scientist, Department of Pediatrics and GA Cancer Center, Children Hospital at GA, Augusta, GA 30913, USA

\* **Correspondence:** Email: [brli1@juno.com](mailto:brli1@juno.com), [bli@augusta.edu](mailto:bli@augusta.edu); Tel: +4403171443.

**Abstract:** To support the study of Krüppel-like factor 2 (KLF2) regulatory mechanisms on cytotoxic T lymphocytes (CTLs), we studied a possibility with a web-based bioinformatics module that enables researchers to identify putative KLF2-binding promoter regions in genomic DNA sequences. After a KLF2 protein structure with C2H2 zinc finger domain and binding-site analysis, we successfully set up a tool to integrate Python-based sequence parsing and motif identification routines to locate CACCC motifs near potential start codons (e.g., ATG) across reading frames associated with key CTL genes such as TNF- $\alpha$  and IFN- $\gamma$ . The tool supports visualization and sequence upload functionality through a static website interface, making it accessible for researchers and clinicians investigating KLF2-mediated transcriptional control in tumor-infiltrating lymphocytes (TILs). This work supplements our primary study on spatial-temporal regulatory networks involved in TIL reactivation by KLF2 down-regulation.

**Keywords:** KLF2; C2H2 zinc finger domain; Omics analysis; T-cells; Tumor-infiltrating lymphocytes (TILs); cytotoxic T lymphocytes (CTLs); quantitative pathway and network; spatial-timely quantitative network (spatial-temporal quantitative network); personalized therapy

---

### **1. Introduction**

Tumor-infiltrating lymphocytes can be applied to kill tumor cells by culturing and infusing them

into patients [1]. Thirty years ago, we established TIL isolated and culture methods from solid tumor tissues so that the earliest adoptive cell therapy (ACT) could be used to eliminate solid cancer [2–7]. Because TIL treatment efficacy is variable for solid tumors or patients, we began to study TIL immune characteristics by isolating the heterogeneous immune cells from solid tumors to study more effective treatment [8]. After thirty years' effort, we have established single-cell isolation from the heterogeneous TILs and analyzed genomics features from the isolated cells, including TIL-CD3, TIL-CD8, TIL-CD4, TIL-NK, and TIL-NKT [9,10]. We now understand that TILs have a distinct killing of tumor cells based on individual immune information from patients [11,12]. To increase the efficacy of immune cell treatment and to discover immune factors for killing tumor cells from individual patients, we establish a TIL CD8 network, such as the TGF-beta pathway, IL-2 activity pathway, and MHC pathway; an NK network from TILs and NKT cells from the TILs. Here, we study the spatial-temporal quantification network for future artificial intelligence (AI) analysis for the next new generation of immunotherapy [13–15].

Spatial-timely quantification network (or spatial-temporal quantification network) is Omics regulation regarding protein-protein, protein-DNA, and protein-RNA (including mRNA, miRNA, lncRNA, and piRNA) in a network. To address the spatial competition of complex proteins, we have reported a spatial-timely quantification network by protein-protein analysis, such as SMAD2/SMAD3/SMAD4 in the TGF-beta pathway and STAT3 complex functions [16,17]. As is known, protein-DNA regulation or protein-RNA regulation also play an important role in spatial-temporal quantification networks. After bioinformatic analysis for KLF2, we set up a web search and then used the web search to study KLF2-DNA downregulation in network regulation.

Our purpose of this research is to set automatically mining downstream motifs, a bioinformatics-based design for known consensus elements for KLF2 binding. This platform enables researchers to explore candidate regulatory regions that mediate KLF2-dependent transcriptional control, thereby supporting hypothesis generation and *in silico* validation ahead of experimental work or to facilitate broader exploration of this regulatory mechanism for future Omics-level regulation in genomic contexts.

## 2. Methods

### 2.1. KLF protein family comparison

Homologous study of the KLF family was performed by the Clustal Omega at the EMBL's European Bioinformatics Institute using the Multiple Sequence Alignment (MSA) program (<https://www.ebi.ac.uk>) as reported in [18]. Sequence comparisons of the protein expression were carried out against all entries at the GenBank database in Homo sapiens (<http://www.ncbi.nlm.nih.gov/index.html>).

### 2.2. Study on the KLF-2 C2H2 zinc finger

An analysis of the KLF2 C2H2 zinc finger domain was performed using KLF family methods with Clustal Omega at the EMBL's European Bioinformatics Institute and using the Multiple Sequence Alignment (MSA) program (<https://www.ebi.ac.uk>) as shown above. KLF-2 C2H2 zinc finger domain sequence comparisons from the GenBank database in Homo sapiens (<http://www.ncbi.nlm.nih.gov/index.html>).

### 2.3. Analyzing the KLF-2 C2H2 Zinc finger DNA-binding site

The KLF2 C2H2 zinc finger DNA-binding site was analyzed for protein structure using the protein structure program. Thereafter, the KLF2 C2H2 zinc finger domain was defined and the C2H2 domain was discovered under the protein structure program (<https://esmatlas.com/>). KLF-2 subtype C2H2 domain primary sequence, secondary structure, and 3D structure were observed from the GenBank database in Homo sapiens in protein (<http://www.ncbi.nlm.nih.gov/index.html>).

### 2.4. Establishing the motif identification algorithm

The KLF2 C2H2 domain primary sequence, secondary structure, and 3D structure were studied, and we confirmed that the KLF2 C2H2 domain can bind the DNA sequence “CACCC”. We began to establish a web-search algorithm, including three steps: (A) Targeting motif; (B) filter criteria; and (C) data integration.

#### 2.4.1. Targeting motif

The Python script (KLF2.py) implemented two major functions: Finding motif positions (sequence, motif) and identifying all occurrences of a target motif (default: “CACCC”) in the input DNA sequence. Finding ATG in frames (sequence, starting codon) entailed scanning the DNA sequence in all three reading frames for specified start codons (default: “ATG”, can include alternatives such as “CTG”). The tool processed user-supplied genomic sequences in a FASTA-like format by removing line breaks and converting characters to uppercase. It then recorded the absolute positions of CACCC motifs and potential start codons.

#### 2.4.2. Filtering criteria

To find promoter candidates, the algorithm filtered CACCC motif locations based on a 500 base-pair distance threshold upstream from each start codon. For each codon, the script checked if any CACCC motif fell within this range, indicating potential promoter functionality. The output included: (A) Last occurrence of each codon; (B) associated CACCC motifs within the threshold; and (C) distance metrics for potential promoter-coding region pairs.

#### 2.4.3. Deployment and Integration

The website was structured as a static HTML interface with CSS styling for layout and presentation. The user uploads or pastes a DNA sequence, selects codon preferences, and initiates the motif scan through the integrated Python backend (or locally emulated in client-side JS for broader access). Results are displayed in real time, with promoter sites and start codons highlighted. All scripts and the sequence processing logic are embedded in the building folder of the web directory, and the tool is integrated into the overall clinical research portal for TIL-based immunotherapy modeling.

### 3. Analysis results

#### 3.1. Results of KLF protein family comparison

To confirm the KLF2 similarity degree in the homologous KLF family from KLF1 to KLF17, a phylogenetic tree generation is used after the ClustalW2 program. The phylogenetic tree of the KLF2 protein is shown in Figure 1. As shown in Figure 1, KLF2 is almost similar to KLF4, so we can decide that KLF4 is selected as the Web-based search control.

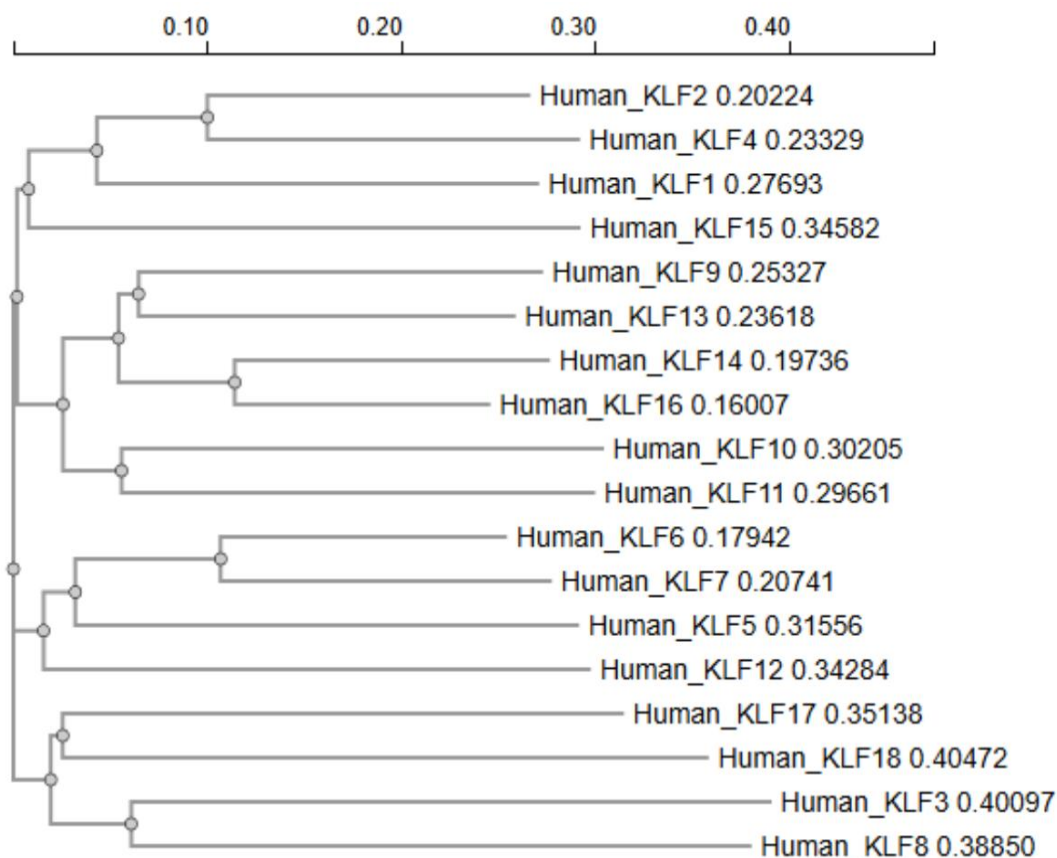


**Fig-1. Alignment for human KLF family**

**Figure 1.** Phylogenetic analysis of the human KLF protein family. Multiple sequence alignment of KLF1–KLF18 is performed with ClustalW2; a distance-based tree is shown with branch lengths indicating sequence divergence. KLF2 clusters closely with KLF4.

#### 3.2. Results of the KLF-2 C2H2 zinc finger

To confirm that the KLF2 C2H2 zinc finger domain can bind a downstream DNA promoter sequence, we studied the KLF2 C2H2 zinc finger domain from homologous KLF family selected from KLF2, KLF4, KLF1, and KLF5. Three C2H2 zinc finger domains were used from the ClustalW2 program and three C2H2 zinc finger domains are produced, as shown in Figure 2. As shown in Figure 2,

three C2H2 zinc finger domains are demonstrated as C-XXXX-C or H-XXXX-H in domain-1, C-XXXX-C or H-XXXX-H in domain-2, and C-XXX-C or H-XXXX-H in domain-3, so that we can further analyze the C2H2 zinc finger domains' binding sequence.

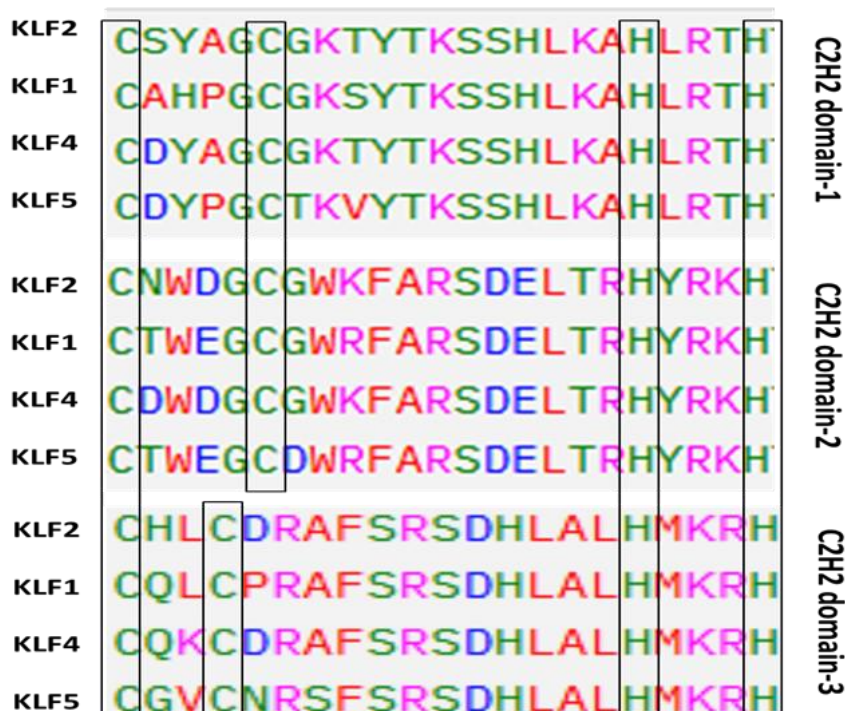


**Fig-2. Alignment for human KLF C2H2 domain**

**Figure 2.** Characterization of KLF2 C2H2 zinc-finger domains. Multiple sequence alignment of homologous KLF proteins (KLF2, KLF4, KLF1, and KLF5) is performed using ClustalW2 to identify conserved zinc-finger motifs. Three conserved C2H2 zinc-finger domains are detected, each displaying the canonical patterns C-X<sub>4</sub>-C and H-X<sub>4</sub>-H (boxed). The alignment highlights residue conservation across the family, supporting that KLF2 contains three typical C2H2 motifs responsible for downstream DNA-binding activity.

### 3.3. Analysis of the KLF-2 C2H2 Zinc finger for the DNA-binding site

After the KLF2 C2H2 zinc finger domain is defined and the C2H2 domain is discovered under the protein structure program (<https://esmatlas.com/>), a secondary structure is shown as in Figure 3A, where the predicted structure is in red, indicating a higher conserved structure (pLDDT < 0.5) for the second structure. We further studied the 3-D structure of the C2H2 with zinc finger domains, which a 3-D structure demonstrates in Figure 3B.

Finally, C2H2 with zinc finger domains in KLF2 were studied to bind the DNA sequence. Moreover, Figure 4A shows the primary sequences from the C2H2 zinc finger zinc as C-XXXX-C and H-XXXX-H in the conserved domain. Figure 4B shows, in 3-D, that C2H2 have exposure bonds, and Figure 4C shows that the exposure bonds can bind downstream DNA CACCC.

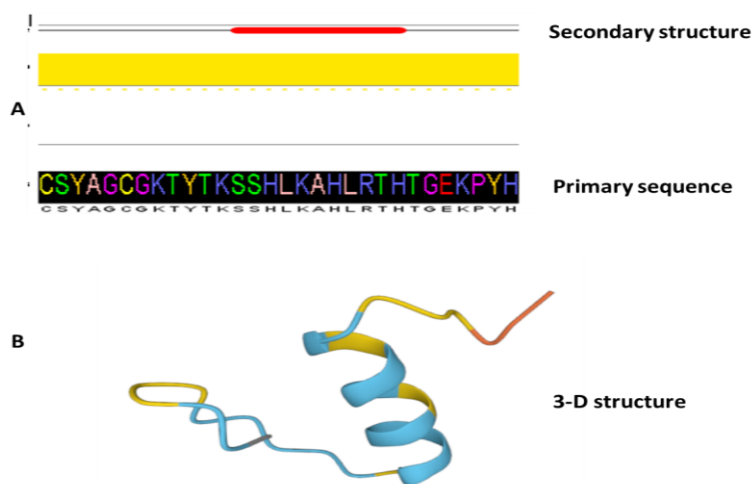


**Fig-3. Human KLF C2H2 domain primary, secondary and 3-D structure**

**Figure 3.** Structural prediction of the KLF2 C2H2 zinc-finger domain. A) Secondary-structure prediction of the KLF2 C2H2 zinc-finger domain generated using the ESM Atlas web server. The red regions indicate residues with higher structural confidence ( $pLDDT > 0.5$ ). B) Predicted 3-D structure of the KLF2 zinc-finger domain showing  $\alpha$ -helices and  $\beta$ -loops typical of C2H2 motifs. The structure illustrates the potential DNA-binding interface within the zinc-finger region.

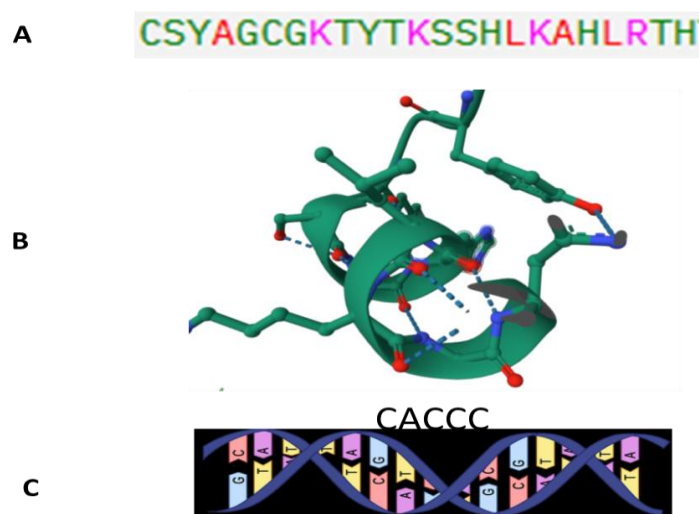


**Fig-4. Human KLF C2H2 domain binding DNA sequences**

**Figure 4.** Predicted DNA-binding interaction of the KLF2 C2H2 zinc-finger domain. A) Primary sequence of the KLF2 C2H2 zinc-finger domain showing the conserved C-X<sub>4</sub>-C and H-X<sub>4</sub>-H motifs that define the zinc-finger structure. B) Three-dimensional model of the C2H2 domain generated by molecular-structure prediction, illustrating the exposed binding interface (highlighted residues) that forms potential hydrogen-bond interactions. C) Schematic representation of the predicted KLF2-DNA interaction, in which the zinc-finger domain recognizes the downstream CACCC consensus sequence within promoter regions.

### 3.4. Establishment of the motif identification algorithm

After we confirmed that the KLF2 C2H2 domain can bind the DNA sequence “CACCC”, we began to establish an algorithm, as demonstrated above, through three steps: (A) Targeting motif; (B) filter criteria; and (C) data integration. Our results show that “CACCC” is defined as a DNA binding-site, which is shown in Figure 5. Some results are reported by experiments, such as the KLF2 binding-promoter sequence [19].

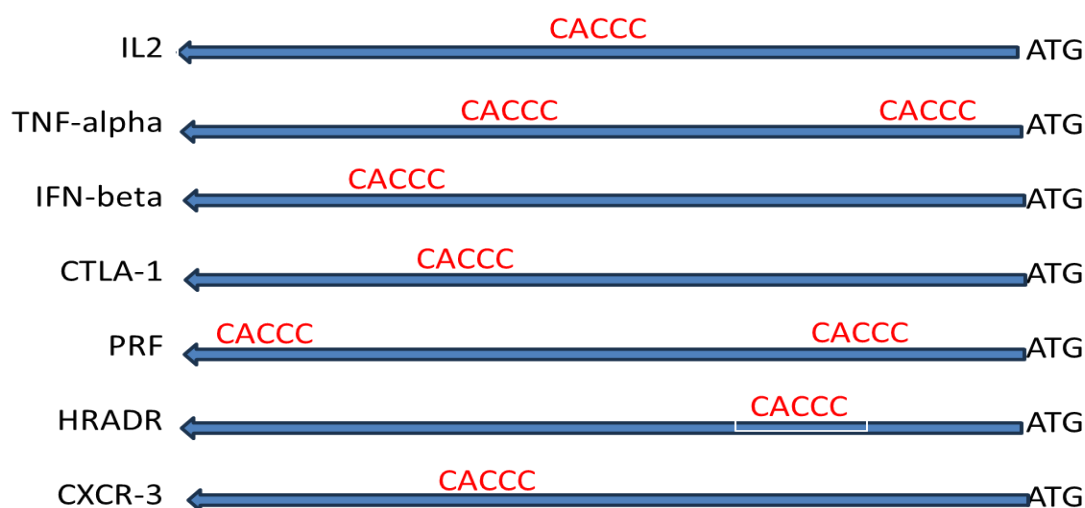


**Fig-5 KLF2 protein CACCC binding site in promoter**

**Figure 5.** Algorithmic workflow for the identification of KLF2 DNA-binding motifs. A) Targeting motif selection step illustrating the identification of CACCC consensus sequences as potential KLF2 binding sites. B) Filtering stage for evaluating motif occurrence and positional relevance within promoter regions. C) Data integration stage combining multiple candidate motifs to define high-confidence KLF2-binding sequences.

Python-based sequence parsing and motif identification, which locates CACCC motifs, is written as notes that will be separately published. We identified upstream CACCC motifs in the promoters of key CTL-related genes (e.g., TNF- $\alpha$ , IFN- $\gamma$ , PRF1, and GrB), as shown in Figure 5, supporting our experimental ChIP and siRNA studies (which will also be reported in a separate manual). Notably, for PRF1, two separate CACCC motifs were located within the defined promoter regions. The tool facilitated rapid silico confirmation of binding regions, significantly reducing the manual effort needed to curate promoter candidates for downstream validation.

## 4. Discussion

KLF2 has been extensively studied as a transcriptional regulator that is critical to maintaining T-cell quiescence and modulating immune effector functions [20–25]. Unsettlingly, KLF2 complex down-regulation has not been discovered in the public KLF2-binding search database. To facilitate

broader exploration of this regulatory mechanism for the future Omics-level, our research plan is to develop an accessible, browser-based interface to identify genomic contexts in which KLF2 may bind downstream CACCC motifs; regulatory elements of CTL effector genes.

We have studied TGF- $\beta$  and STAT3 spatial-temporal quantitative pathways in TILs [16,17,26–30], because the TGF- $\beta$  pathway has two signaling systems: Either the SMAD signaling pathway or the non-SMAD signaling pathway. In SMAD regulation, such as SMAD2 and SMAD3, SMAD4 binds with the phosphorylated SMAD2 and SMAD3 to produce a heterotrimeric transcription complex, which transfers the signal to the nucleus to perform a transcription function called TGF- $\beta$ /SMAD signaling [31], while the SMAD-independent pathway of the TGF- $\beta$  pathway proceeds through RHO GTPases, the RAS pathway, P38 pathway, and mTOR pathway according to research [32]. The dynamic TGF- $\beta$ -inducing phosphorylation of Smad2 and Smad3 needs IP experiments with mass spectrometry [33]. Some scientists showed 84 possible combination regulations, including timely and spatial ones [34]. We set up a spatial-timely quantitation pathway for protein-protein regulation to achieve maximal spatial-timely combination regulation with activity of the SMAD protein-protein complex, with 15,625 combination regulations, so that bioinformatics analysis is more powerful than IP with mass spectrometry analysis [35]. Because the SMAD protein complex in the TGF- $\beta$  spatial-timely quantitative pathway is used only for protein-protein regulation, they cannot differ in protein/DNA binding to support the spatial-timely quantitative network at protein-DNA regulation. Here, we use KLF2 *in silico* to study the protein-DNA modules.

This research contains the first analysis to characterize the KLF2 binding mechanism, such as the KLF2 primary sequence with a phylogenetic tree [36]. Furthermore, to study the KLF2 C2H2 zinc finger domain, we also identified three C2H2 zinc finger domains [37] after the KLF2 C2H2 zinc finger domain was discovered under the protein structure with bonding analysis. Finally, C2H2 with zinc finger domains in KLF2 demonstrated KLF2 C2H2 domain binding to the downstream DNA sequence as CACCC, which has been researched by experiments from our laboratory and other reports [38].

After we confirmed that the KLF2 C2H2 domain can bind the DNA sequence “CACCC”, we established a web-search system (which will be separately published as computer notes). Finally, we successfully used the web-search to identify downstream CACCC motifs in the promoters of key CTL-related genes (e.g., TNF- $\alpha$ , IFN- $\gamma$ , PRF1, and GrB), supporting our experimental ChIP and siRNA studies. The tool facilitated the discovery of binding regions, significantly reducing many miscellaneous experiments.

## 5. Conclusion

TIL has clinical applications by TIL infusion *in vivo* for immune therapy and by TIL analysis *ex vivo* to determine the immune characteristics of tumor patients [39–45]. We have been studying personalized TIL therapy and analyzing other immune therapies from genomics profiles based on TILs and primary tumor cells [46,47]. Although the spatial-timely quantitative network is a more powerful evaluation than current mass spectrometry for protein-protein regulation [16–17], the KLF2 web tool provides an identification of protein-DNA promoter regions that may mediate KLF2 transcriptional repression or activation in CTL genes. In the future, a spatial-timely quantitative network, including protein-protein, protein-DNA, and protein-RNA, can support direct evaluation to apply for Omics' AI analysis.

## Use of AI tools declaration

The authors declare they have not used Artificial Intelligence (AI) tools in the creation of this article.

## Conflicts of interest

Biaoru Li is a member of the editorial board of the *Allergy and Immunology* and was not involved in the editorial review or the decision to publish this article. The authors declare no conflict of interest.

## Author contributions

CWD (1) performs *in silico* experiments and WQL experimental fields, including biostatistics. BL conceived and designed the experiments.

## Acknowledgments

With the support of Dr. H. D. Preisler, we have set up a method to analyze genomic profiles of CD3, CD4, and CD8 from TIL. This work was supported by National Cancer Institute IRG-91-022-09, USA (to BL).

## References

1. Rosenberg SA, Spiess P, Lafreniere R (1986) A new approach to the adoptive immunotherapy of cancer with tumor-infiltrating lymphocytes. *Science* 233: 1318–1321. <https://doi.org/10.1126/science.3489291>
2. Li B, Tong SQ, Zhang XH, et al. (1994) A new experimental and clinical approach of combining usage of highly active tumor-infiltrating lymphocytes and highly sensitive antitumor drugs for the advanced malignant tumor. *Chin Med J (Engl)* 107: 803–807.
3. Li B, Tong SQ, Zhang XH, et al. (2020) Chapter 9: Development of adoptive T-cell immunotherapy: Future of personalized immunotherapy, In: *Personalized Immunotherapy for Tumor Diseases and Beyond*, Sharjah: Bentham Science, 137–154. <https://doi.org/10.2174/9789811482755120010012>
4. Hu BC, Li GW, Wei C, et al. (1997) Clinical application of infiltrating lymphocytes in malignant brain tumors. *J Immunol* 2: 1–2.
5. Hua ZD, Lu J, Li HF, et al. (1996) Clinical study of tumor-infiltrating lymphocytes in ovarian cancer. *Chin J Obstet Gynecol* 31: 55–57.
6. Lu J, Hu LW, Hua ZD, et al. (1996) Analysis of the therapeutic effects of different therapeutic approaches for TIL. *Chin J Cancer Biother* 3: 127–129.
7. Cai XM, Lu J, Hua ZD, et al. (1996) Clinical application of TIL from different sources. *J Immunol* 12: 251–254.
8. Li B, Ding J, Larson A, et al. (1999) Tumor tissue recycling—A new combination treatment for solid tumors: Experimental and preliminary clinical research. *In Vivo* 13: 433–438.

9. Zhang W, Ding J, Qu Y, et al. (2009) Genomic expression analysis of quiescent CD8 T-cells from tumor-infiltrating lymphocytes of *in vivo* liver tumor by single-cell mRNA differential display. *Immunology* 127: 83–90. <https://doi.org/10.1111/j.1365-2567.2008.02926.x>
10. Xu YB, Hu HL, Zheng J, et al. (2013) Feasibility of whole RNA sequencing from single-TIL cell mRNA amplification. *Genet Res Int* 724124. <https://doi.org/10.1155/2013/724124>
11. Li B, Hu HL, Ding J, et al. (2015) Functional cell-proliferation and differentiation by system modeling for cell therapy. *IJLSRST* 4: 180–187.
12. Ying XN, Li B (2022) Machine-learning modeling for personalized immunotherapy—An evaluation module. *Biomed J Sci Tech Res* 47: 38211–38216.
13. Li B (2005) A strategy to identify genomic expression profiles at the single-T-cell level and a small number of cells. *J Biotechnol* 8: 71–81. <https://doi.org/10.2225/vol8-issue1-fulltext-3>
14. Li B, Perabekam S, Liu G, et al. (2002) Experimental and bioinformatics comparison of gene expression between T cells from TIL of liver cancer and T cells from unigene. *J Gastroenterol* 37: 275–282. <https://doi.org/10.1007/s005350200035>
15. Li B (2000) Identification of mRNAs expressed in tumor-infiltrating lymphocytes by a strategy for rapid and high-throughput screening. *Gene* 255: 273–279. [https://doi.org/10.1016/S0378-1119\(00\)00330-9](https://doi.org/10.1016/S0378-1119(00)00330-9)
16. Yang Y, Li WQ, Chen SY, et al. (2023) Spatial-timely quantitative network analysis for TGF- $\beta$  pathway of tumor infiltrating lymphocytes. *J of Cancer Sci Cancer Ther* 7: 194–294. <https://doi.org/10.22541/au.169454708.84070919/v1>
17. Yang Y, Chen SY, Li WQ, et al. (2025) STAT3 down-regulation for IL-2 inducing TIL-A clinical clue for spatial quantitative pathway analysis. *AIMS Allergy Immunol* 8: 283–295. <https://doi.org/10.3934/Allergy.2024017>
18. Sievers F, Higgins DG (2018) Clustal Omega for making accurate alignments of many protein sequences. *Protein Sci* 27: 135–145. <https://doi.org/10.1002/pro.3290>
19. Anderson KP, Kern CB, Crable SC, et al. (1995) Isolation of a gene encoding a functional zinc finger protein homologous to erythroid Kruppel-like factor: Identification of a new CACCC-box binding protein. *Mol Cell Biol* 15: 5957–5965. <https://doi.org/10.1128/MCB.15.11.5957>
20. Kuo CT, Veselits ML, Leiden JM (1997) LKLF: A transcriptional regulator of single-positive T cell quiescence and survival. *Science* 277: 1986–1990. <https://doi.org/10.1126/science.277.5334.1986>
21. Carlson CM, Endrizzi BT, Wu JH, et al. (2006) Kruppel-like factor 2 regulates thymocyte and T-cell migration. *Nature* 442: 299–302. <https://doi.org/10.1038/nature04882>
22. Buckley AF, Kuo CT, Leiden JM (2001) Transcription factor LKLF is required for T-cell homeostasis and quiescence. *Curr Opin Immunol* 13: 354–360.
23. Schober SL, Kuo CT, Schluns KS, et al. (1999) Expression of the transcription factor Kruppel-like factor 2 enhances the survival of naive T cells. *Immunity* 11: 759–769.
24. Preston GC, Feijoo-Carnero C, Schurch N, et al. (2013) The impact of KLF2 on the transcriptional program and cell cycle of quiescent CD8<sup>+</sup> T cells. *PLoS One* 8: e77584. <https://doi.org/10.1371/journal.pone.0077537>
25. Weinreich MA, Takada K, Skon CN, et al. (2009) KLF2 transcription-factor deficiency in T cells results in unrestrained cytokine production and enhanced effector differentiation. *J Immunol* 182: 6641–6649. <https://doi.org/10.1016/j.immuni.2009.05.011>
26. Qin HR (2012) Roles of STAT3 and SMAD3 signaling in human T cells: Functional interaction and transcriptional cross-regulation. *J Biol Chem* 287: 3623–3631.

27. Wang T, Niu G, Kortylewski M, et al. (2004) Regulation of the innate and adaptive immune responses by Stat3. *Nat Med* 10: 48–54. <https://doi.org/10.1038/nm976>
28. Shi Y, Massagué J (2003) Mechanisms of TGF- $\beta$  signaling from cell membrane to the nucleus. *Cell* 113: 685–700. [https://doi.org/10.1016/S0092-8674\(03\)00432-X](https://doi.org/10.1016/S0092-8674(03)00432-X)
29. Moustakas A, Heldin CH (2005) Non-SMAD TGF- $\beta$  signals. *J Cell Sci* 118: 3573–3584. <https://doi.org/10.1242/jcs.02554>
30. Wrighton KH, Lin X, Feng XH (2009) Phospho-control of TGF- $\beta$  superfamily signaling. *Cell Res* 19: 8–20. <https://doi.org/10.1038/cr.2008.327>
31. Schmierer B, Hill CS (2007) TGF $\beta$ –SMAD signal transduction: molecular specificity and functional flexibility. *Nat Rev Mol Cell Biol* 8: 970–982. <https://doi.org/10.1038/nrm2297>
32. He K, Zhang J, Chen J, et al. (2020) Computational modeling of dynamic TGF- $\beta$  signaling reveals combinatorial regulation mechanisms. *PLoS Comput Biol* 16: e1008191.
33. Pearson JC, Lemons D, McGinnis W (2005) Comparison of the mammalian and *Drosophila* Hox gene complexes suggests functional conservation of regulatory circuits. *Proc Natl Acad Sci USA* 102: 4576–4581.
34. Pavletich NP, Pabo CO (1991) Zinc finger–DNA recognition: Crystal structure of a Zif268–DNA complex at 2.1 Å. *Science* 252: 809–817. <https://doi.org/10.1126/science.2028256>
35. Anderson KP, Kern CB, Crable SC, et al. (1995) Isolation of a gene encoding a functional zinc finger protein homologous to erythroid Kruppel-like factor: Identification of a new CACCC-box binding protein. *Mol Cell Biol* 15: 5957–5965. <https://doi.org/10.1128/MCB.15.11.5957>
36. ENCODE Project Consortium (2012) An integrated encyclopedia of DNA elements in the human genome. *Nature* 489: 57–74. <https://doi.org/10.1038/nature11247>
37. Kent WJ, Sugent CW, Furey TS, et al. (2002) The human genome browser at UCSC. *Genome Res* 12: 996–1006. <https://doi.org/10.1101/gr.229102>
38. Batlle E, Massagué J (2019) Transforming growth factor- $\beta$  signaling in immunity and cancer. *Immunity* 50: 924–940. <https://doi.org/10.1016/j.immuni.2019.03.024>
39. Rosenberg SA, Yang JC, Sherry RM, et al. (2011) Durable complete responses in heavily pretreated patients with metastatic melanoma using T-cell transfer immunotherapy. *Clin Cancer Res* 17: 4550–4557. <https://doi.org/10.1158/1078-0432.CCR-11-0116>
40. Dudley ME, Wunderlich JR, Shelton TE, et al. (2003) Generation of tumor-infiltrating lymphocyte cultures for use in adoptive transfer therapy for melanoma patients. *J Immunother* 26: 332–342. <https://doi.org/10.1097/00002371-200307000-00005>
41. Radvanyi LG, Bernatchez C, Zhang MY, et al. (2012) Specific lymphocyte subsets predict response to adoptive cell therapy using expanded autologous tumor-infiltrating lymphocytes in metastatic melanoma patients. *Clin Cancer Res* 18: 6758–6770. <https://doi.org/10.1158/1078-0432.CCR-12-1177>
42. Van der Leun AM, Thommen DS, Schumacher TN (2020) CD8<sup>+</sup> T cell states in human cancer: Insights from single-cell analysis. *Nat Rev Cancer* 20: 218–232. <https://doi.org/10.1038/s41568-019-0235-4>
43. Sade-Feldman M, Yizhak K, Bjorgaard SL, et al. (2018) Defining T cell states associated with response to checkpoint immunotherapy in melanoma. *Cell* 175: 998–1013.e20. <https://doi.org/10.1016/j.cell.2018.10.038>

44. Thommen DS, Koelzer VH, Herzig P, et al. (2018) A transcriptionally and functionally distinct PD-1<sup>+</sup>CD8<sup>+</sup> T cell pool with predictive potential in non-small-cell lung cancer treated with PD-1 blockade. *Nat Med* 24: 994–1004. <https://doi.org/10.1038/s41591-018-0057-z>
45. Tran E, Robbins PF, Lu YC, et al. (2016) T-cell transfer therapy targeting mutant KRAS in cancer. *N Engl J Med* 375: 2255–2262. <https://doi.org/10.1056/NEJMoa1609279>
46. Li B (2024) Surgery and specimen biobanks—Tumor tissues and precision medicine. *J Surg* 9: 11108.
47. Huang XH, Lu J, Zhang YF, et al. (2024) Prediction, Prevention, prognostic and personalized therapy of ovarian cancer- biomarkers and precision medicine. *Biomed J Sci Tech Res* 83: 223–231.



AIMS Press

© 2026 the Author(s), licensee AIMS Press. This is an open access article distributed under the terms of the Creative Commons Attribution License (<https://creativecommons.org/licenses/by/4.0>)